Journal of Alloys and Compounds 520 (2012) 122–126

Contents lists available at SciVerse ScienceDirect

Journal of Alloys and Compounds

journal homepage: www.elsevier.com/locate/jallcom

Crystal growth, magnetic and transport properties of single-crystal YbCuGe

Kenichi Katoh[a,*], Masafumi Maeda[a], Saori Matsuda[b], Akira Ochiai[b]

[a] Department of Applied Physics, National Defense Academy, Yokosuka, Kanagawa 239-8686, Japan
[b] Department of Physics, Tohoku University, Sendai 980-8578, Japan

ARTICLE INFO

Article history:
Received 2 December 2011
Received in revised form
28 December 2011
Accepted 28 December 2011
Available online 8 January 2012

Keywords:
Magnetically ordered materials
Rare earth alloys and compounds
Crystal growth
Electrical transport
Magnetization

ABSTRACT

The magnetic and transport properties of single-crystal of YbCuGe are presented. The magnetic susceptibility which shows uniaxial anisotropic behavior along the *c*-axis in all temperature range has a kink at around 4.2 K. The specific heat also shows a λ-type peak at 4.2 K, which moves toward low temperature side by an application of the magnetic field up to 90 kOe. The linear specific heat coefficient is estimated to be 5.2 mJ/mol K^2 from the zero field data. The electrical resistivity for the current along the principal axes shows a metallic behavior with a broad maximum at around 200 K. The Hall coefficient drastically changes from the negative minimum at 70 K to the positive constant value below 10 K. These results indicate that YbCuGe is a metallic antiferromagnet with T_N = 4.2 K.

1. Introduction

Unusual ground states of the Ce-based compounds which have attracted many researchers are considered to be linked to the competition between the Kondo effect and the Ruderman–Kittel–Kasuya–Yosida (RKKY) interaction through the hybridization between *f*-electrons and conduction electrons [1]. The variety of physical properties observed in Ce-based compounds pushes forward the investigation of Yb systems, because of symmetric relationship between one 4*f*-hole of the trivalent Yb ion and one 4*f*-electron of the trivalent Ce ion. Especially the physical properties of a series YbTX (T = transition metal, and X = element of the 3rd or 4th main group) are well investigated in the last three decades [2]. In recent years, we have attempted to reveal physical properties of YbCuGe, YbRhGe, YbAgGe, YbIrGe, and YbPtGe because of their unclear physical properties [3–6]. Among them, we revealed that YbPtGe is a middle-classed heavy-fermion ferromagnet with the Curie temperature T_C = 5.4 K. In general, the magnetic field of the spontaneous magnetization below T_C may suppress the Kondo interaction which makes a spin-singlet composed of *f* and conduction electrons. We consider that the study of 4*f*-hole based heavy fermion state in ferromagnet may lead the new aspect of the Kondo effect different from that in the 4*f*-electron system. While YbNiSn is well known as a heavy-fermion ferromagnet with T_C = 5.65 K, the obtained single crystal is too small and coarse to investigate this subject [7,8]. To proceed with a study of heavy-fermion state in ferromagnet, we aimed at ferromagnetic properties of YbCuGe from the results of a sudden rise of the magnetic susceptibility below 8 K and a saturated magnetization of 0.7μ_B/formula unit which is estimated from a plot of $M(H)$ vs. the inverse field $1/H$ extrapolating to $1/H = 0$. In the hexagonal LiGaGe-type structure of YbCuGe with the space group $P6_3mc$, Yb atoms align along the *c*-axis in the honeycomb tube composed of Cu and Ge atoms [9]. The strongly anisotropic behavior will be expected in the magnetic and electrical properties as reported in the isostructural ferromagnet CePdSb and CePtSb [10]. In this paper, we will present the crystal growth, magnetic susceptibility, magnetization, electrical resistivity, transverse magnetoresistivity, Hall coefficient, and specific heat of single-crystal of YbCuGe and its reference compound LuCuGe.

2. Experimental procedure

Single crystal of YbCuGe was obtained by the Bridgman method using a sealed tungsten crucible. Polycrystalline of LuCuGe was prepared by arc-melting with equiatomic composition and annealing at 750 °C for one week. The purities of the starting materials were 99.9% for Yb and Lu, 99.99% for Cu, and 99.999% for Ge, respectively. At first, an alloy composed of Cu and Ge with an adequate ratio was prepared by arc-melting in purified argon atmosphere of 99.9999%. This alloy and Yb lump were loaded in the tungsten crucible and sealed in vacuum using an electron beam welder. To grow a single crystal, the crucible was hold in a stable high-temperature for one hour in electric furnace and then pulled down from heater at a rate of 2 mm/h.

A single crystal of YbCuGe with 6 mm in diameter, which is sparkling in yellow-green, was obtained from the conditions of a ratio of Yb:Cu:Ge = 5:5:6 and 1430 °C. We have prepared only fragile crystal less than a size of 1 mm radius from the condition of the stoichiometric composition in heating temperature up to 1440 °C.

* Corresponding author. Tel.: +81 46 841 3810; fax: +81 46 844 5912.
E-mail address: katok@nda.ac.jp (K. Katoh).

0925-8388/$ – see front matter © 2012 Elsevier B.V. All rights reserved.
doi:10.1016/j.jallcom.2011.12.147

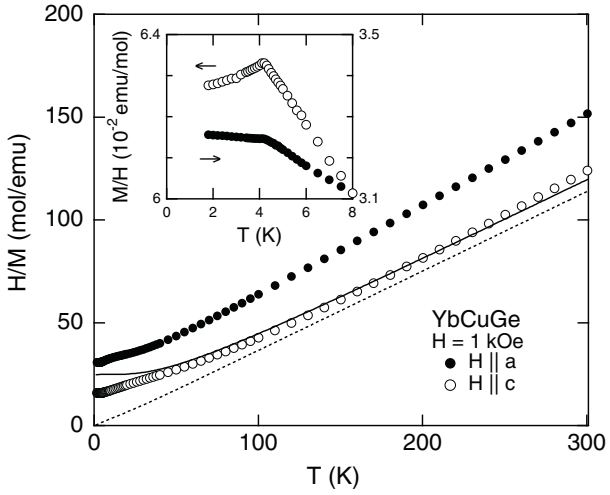

Fig. 1. Temperature dependence of the inverse magnetic susceptibility measured at applied magnetic field of 1 kOe along the *a*- and *c*-axes of YbCuGe. Solid and dashed lines are the calculated results for the *a*- and *c*-axes, respectively. The inset shows the temperature dependence of the magnetic susceptibility below 8 K.

While no impurity phase in YbCuGe was detected from the X-ray powder diffraction measurement, LuCuGe alloy includes a few amount of $Lu_3Cu_4Ge_4$. The lattice parameters obtained from the X-ray patterns between $2\theta = 20^\circ$ and 100° are $a = 4.219$ Åand $c = 7.068$ Åfor YbCuGe, and $a = 4.215$ Åand $c = 6.980$ Åfor LuCuGe, respectively.

Magnetic properties were measured using a commercial superconducting quantum interference device (SQUID) magnetometer (MPMS-5 of Quantum Design Inc., USA) in the temperature range between 1.9 and 300 K at magnetic fields of up to 50 kOe. The measured samples were shaped to a size of 2.0–2.5 mm cube. Transport property measurements were performed using a commercial instrument (PPMS-9 of Quantum Design Inc., USA) from 300 down to 1.9 K. Electrical resistivity was measured by a standard four-probe dc technique using rectangular sample with a thickness of 0.5 mm. To detect the Hall voltage, ac technique with current of 30 mA and 20 Hz was adopted to sample with a thickness of 0.35 mm in application of magnetic field of 10 kOe.

3. Experimental results

Fig. 1 shows the temperature dependence of the inverse magnetic susceptibility $1/\chi(T)$ of YbCuGe at $H = 1$ kOe for $H \parallel a$ $(1/\chi_a)$ and $H \parallel c$ $(1/\chi_c)$. Uniaxial anisotropic behavior along the *c*-axis is clearly observed. Above 100 K, each $1/\chi(T)$ data point for $H \parallel a$ and $H \parallel c$ obeys the Curie–Weiss law. The obtained Weiss-temperature θ_p and effective magnetic moment μ_{eff} are $\theta_p = -44.8$ K, $\mu_{eff} = 4.27\mu_B$ for $H \parallel a$, and $\theta_p = -0.94$ K, $\mu_{eff} = 4.43\mu_B$ for $H \parallel c$, respectively. These values of μ_{eff} are close to the value of $4.53\mu_B$ expected for the free Yb^{3+} ion. θ_p for $H \parallel a$ is considerably less than that for $H \parallel c$. We consider that this magnetic anisotropy in the higher-temperature range is ascribed to the crystalline electric field (CEF) effect on a single Yb ion. As decreasing temperature below 100 K, χ_a and χ_c form the shoulder and peak structures at 4.2 K as shown in the inset of Fig. 1. It is suggested that the antiferromagnetic ordering occurs below 4.2 K, instead of the ferromagnetic ordering at 8 K in previous report.

The magnetic field dependences of the magnetization $M(H)$ of YbCuGe in the magnetic fields of up to 50 kOe along the *a*- and *c*-axes are shown in Fig. 2. The plotted data is the results measured in the sequence of increasing magnetic field. The $M(H)$ for both $H \parallel a$ (M_a) and $H \parallel c$ (M_c) below 8 K linearly increase with increasing magnetic field up to 50 kOe. The slope at 2 K is 0.57×10^{-2} for $H \parallel a$, and $1.1 \times 10^{-2}\mu_B$/kOe for $H \parallel c$, respectively. The solid line is the data points connected by straight line, which were measured at 2 K in the sequence of decreasing magnetic field from 50 kOe. The data in increasing magnetic field is in good agreement with that in decreasing magnetic field. No hysteresis is consistent to the antiferromagnetic ordering below 4.2 K.

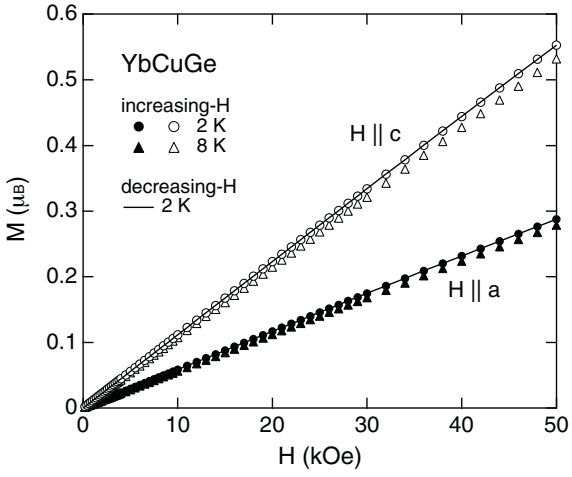

Fig. 2. Field dependences of the magnetization at several fixed temperatures for increasing magnetic fields along the *a*- and *c*-axes of YbCuGe. The solid line is the data measured at 2 K in the sequence of decreasing magnetic field.

The anisotropic temperature dependence of the electrical resistivity $\rho(T)$ of YbCuGe between $I \parallel a$ (ρ_a) and $I \parallel c$ (ρ_c) is shown in Fig. 3. The ρ_a and ρ_c make a broad maximum at around 200 K and decrease rapidly with decreasing temperature in contrast to the linear decrease in the $\rho(T)$ of the nonmagnetic counterpart LuCuGe. These $\rho(T)$ anomalies at approximately 200 K are probably attributable to the CEF population effects rather than the Kondo effect as discussed later. Both ρ_a and ρ_c monotonously decrease below 10 K and show no anomaly at around 4 K where $\chi(T)$ makes hump as shown in the inset of Fig. 3. The normalized transverse magnetoresistivity $\Delta\rho_H(H)/\rho_H(0)$, where $\Delta\rho_H(H)$ is calculated by $(\rho_H(H) - \rho_H(0))/\rho_H(0)$, at 2 K is shown in Fig. 4. $\Delta\rho_H(H)/\rho_H(0)$ of LuCeGe has a field variation with power law of $H^{1.3}$ as indicated in the solid curve. However, $\Delta\rho_H(H)/\rho_H(0)$ of YbCeGe for each direction shows weak dependence for field. An increase proportional to H^2 in $\Delta\rho_H(H)/\rho_H(0)$ implies that compensated metal with no open orbits, or uncompensated metal with open orbit direction which is parallel to the current direction [11]. While the rather large residual resistivity may be related to this gradual increase of $\Delta\rho_H(H)/\rho_H(0)$

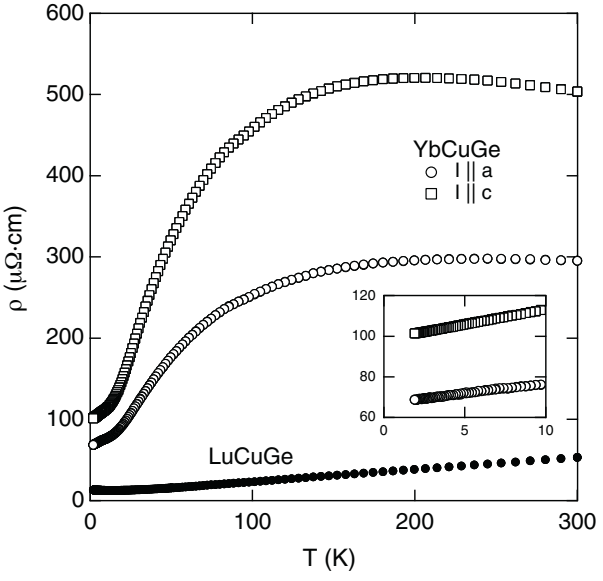

Fig. 3. Temperature dependences of the electrical resistivity along the *a*- and *c*-axes of YbCuGe, and that for LuCuGe. The inset shows the expanded data below 10 K.

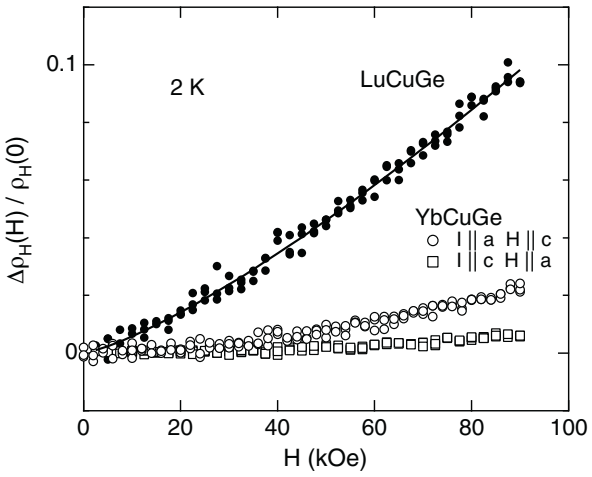

Fig. 4. Field dependences of the normalized transverse magnetoresistivity at 2 K along the *a*- and *c*-axes of YbCuGe, and that for LuCuGe. The solid curve is a fitting result.

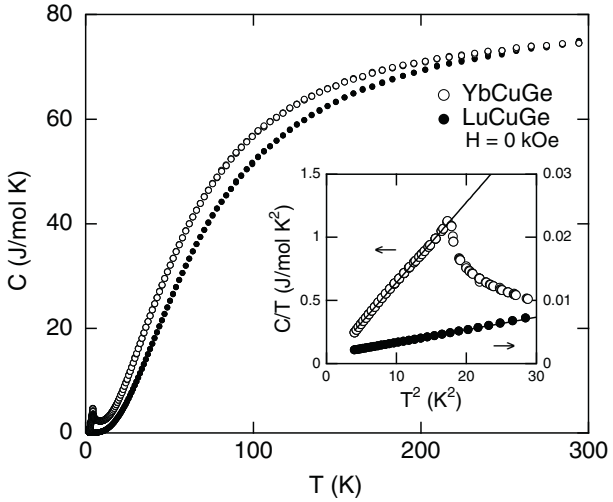

Fig. 6. Temperature dependences of the specific heat for YbCuGe and LuCuGe. The inset shows the specific heat divided by temperature vs the square of the temperature plots.

for each current direction, there is a possibility that YbCuGe is a uncompensated metal with no open orbit.

Fig. 5 shows the temperature dependences of the Hall coefficient $R_H(T)$ of YbCuGe for $I \parallel a$ ($H \parallel c$) and $I \parallel c$ ($H \parallel a$) including that of LuCuGe. With decreasing temperature, $R_H(T)$ for each current of YbCuGe shows the negative minimum at around 70 K and changes to the positive constant value. Below 20 K, $R_H(T)$ for $I \parallel a$ makes a broad maximum at 8 K, while that for $I \parallel c$ saturates to a constant value down to 1.9 K. Any anomaly at around 4.2 K is not found in both $R_H(T)$. The carrier concentration is estimated to be 0.1 hole/f.u. from the value of 3.3×10^{-3} cm^3/C for $R_H(T)$ of $I \parallel c$ at 2 K. On the contrary, $R_H(T)$ of LuCuGe is almost independent for temperature. The carrier concentration is 0.35 hole/f.u. estimated from the value of 9.5×10^{-4} cm^3/C at 2 K. Because of the fairly different dependence of $R_H(T)$ between YbCuGe and LuCuGe, the extraordinary Hall effect proportional to the magnetization is possible to explain the drastic temperature-variation of $R_H(T)$ of YbCuGe. However, the temperature variation of $R_H(T)$ for $H \parallel c$ is even less than that for $H \parallel a$ contrary to the relation of $\chi_c > \chi_a$. Furthermore, as shown in the inset of Fig. 5, both the Hall resistivity ρ_{xy} for current direction increase linearly with nearly same slope against increasing field up to 90 kOe in spite of the strongly anisotropic $M(H)$. Therefore,

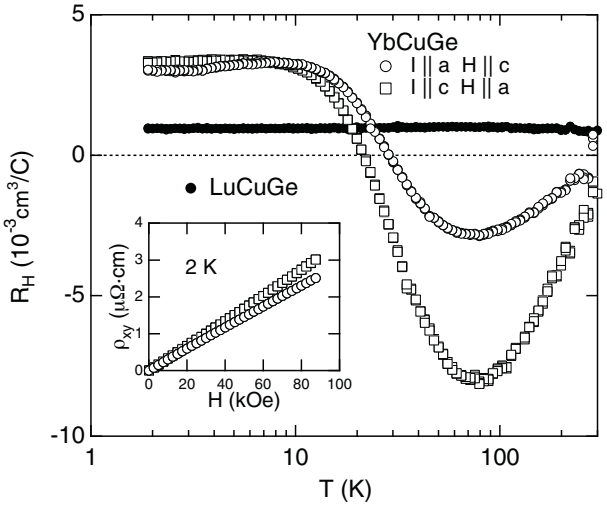

Fig. 5. Temperature dependences of the Hall coefficient for YbCuGe and LuCuGe. The inset shows the field dependence of the Hall resistivity of YbCuGe at 2 K.

it is proposed that the $R_H(T)$ in YbCuGe is mainly ascribed to the ordinary Hall effect as observed in In and Al [12].

The temperature dependences of the specific heat $C(T)$ of YbCuGe and LuCuGe in the magnetic field $H = 0$ kOe are shown in Fig. 6. The $C(T)$ of YbCuGe exhibits a λ-type peak at the Néel temperature $T_N = 4.2$ K instead of 8 K as expected temperature at which ferromagnetic transition may occurs in the previous report [3]. Furthermore, $C(T)$ above T_N shows a minimum at around 10 K compared to gradual increase of that for LuCuGe as lattice contribution. The inset of Fig. 6 shows the $C(T)/T$ vs. T^2 plots at low temperatures. The $C(T)/T$ of LuCuGe follow the formula $C(T)/T = \gamma + \beta T^2$ below $T^2 = 10$ K^2, where the first and second terms represent the electronic and phonon contributions to specific heat, respectively. The estimated γ and β are 1.35 mJ/mol K^2 and 0.199 mJ/mol K^4, respectively. The Debye temperature θ_D is also estimated to be 308 K from the formula $\beta = (12\pi^4/5)ZR/{\theta_D}^3$, where Z, the number of atoms in formula unit, is 3 and R is the gas constant. For YbCuGe, the $C(T)$ below T_N is consistent with a three-dimensional antiferromagnetic magnon law [13]. γ and β are estimated to be 5.23 mJ/mol K^2 and 63.6 mJ/mol K^4 from the data below 4.1 K. The large β value is more than 300 times of that for LuCuGe. Thus, the magnetic contribution due to antiferromagnetic magnon dispersion is predominant over phonon contribution.

Fig. 7 shows the field variation of the magnetic contribution $C_m(T)$ of the specific heat for YbCuGe up to 90 kOe, where $C_m(T)$ is estimated by subtracting that of LuCuGe. The magnetic field is applied along the *c*-axis. By applying a magnetic field, the sharp peak of $C_m(T)$ at 4.2 K decays and shifts to a lower temperature side in contrast to the unmovement of the broad peak at 50 K. The higher peak is ascribed to the Schottky contribution which is derived from four Kramer's doublets for the total angular momentum $J = 7/2$ of Yb^{3+} ion. This peak height of 7 J/mol K is twice of 3.6 J/mol K which is the height of the Schottky peak expected for the excitation between the doublet and another doublet. Later, we attempt to reproduce this broad peak by the Schottky contribution.

The inset of Fig. 7 shows the magnetic contribution $S_m(T)$ for $H = 0$ kOe to the entropy, which is calculated by integrating $C_m(T)/T$ with respect to T. The absence of $C_m(T)$ data below 1.9 K is substituted by the difference between the calculated data $C(T)$ of YbCuGe and LuCuGe using the formula $C(T) = \gamma T + \beta T^3$, where γ and β are estimated in the previous. $S_m(T)$ gradually increases and exceeds Rln2 above 20 K. $S_m(T)$ at T_N is 28% of that of Rln2, expected for a doublet ground state. It is suggested that the slow release of magnetic

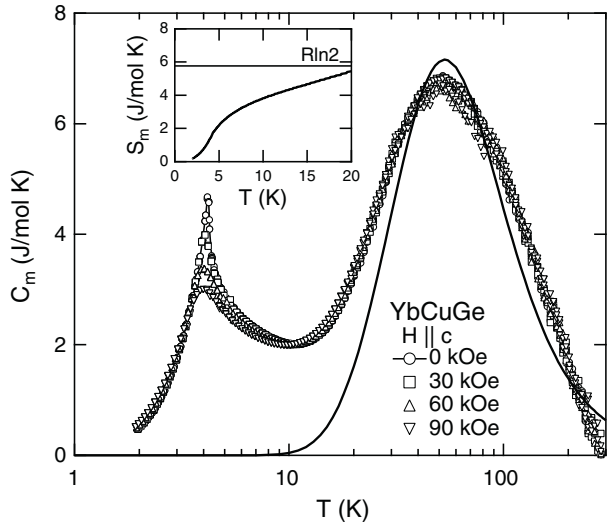

Fig. 7. Temperature dependences of the magnetic contribution of the specific heat for YbCuGe. Solid line is a result of fitting. The inset shows the magnetic entropy for 0 kOe.

entropy is probably ascribed to the spin fluctuation instead of the Kondo effect because of the small γ value, as discussed later.

4. Discussion

At first, we have attempted to explain the relation between the broad peak of $C_m(T)$ centered at 50 K and the anisotropy of $\chi(T)$ for YbCuGe in the paramagnetic state on the basis of the CEF theory. As the characteristic feature of the LiGaGe-type crystal structure, all Yb atoms align along the *c*-axis surrounded by a honeycomb tube formed by Cu and Ge atoms [9]. Then, we determined that the quantization *x*- and *z*-axes on the CEF tensor are parallel to the crystallographic *a*- and *c*-axes, respectively. The CEF Hamiltonian for the trigonal symmetry consists of six terms of the second, fourth, and sixth orders [14]. We treated only the second- and fourth-order terms $B_2^0O_2^0$, $B_4^0O_4^0$, and $B_4^3O_4^3$ on a trial, where B_l^m and O_l^m are the CEF parameters and the Stevens operators, respectively. Because the uniaxial anisotropy of $\chi(T)$ in the experimental results is so large that we preferentially reproduced the broad peak of $C_m(T)$ centered at 50 K. Then, we found the CEF parameters of $B_2^0 = -0.7$ K, $B_4^0 = 0.15$ K, and $B_4^3 = 0.5$ K. The first-, second-, and third-excitation energies of the CEF levels from the ground state were estimated to be 99, 162, and 219 K, respectively. The broad peak of $C_m(T)$ at 50 K could be explained by the calculated Schottky anomaly for this CEF level scheme, as shown by the solid line in Fig. 7. We also show the calculated $\chi^{-1}(T)$ for the *a*- and *c*-axes from the obtained CEF parameters as the solid and dashed lines in Fig. 1, respectively. While the easy axis of the *c*-axis at low temperatures is illustrated, the uniaxial anisotropy of $\chi(T)$ above 100 K is hardly reproduced by the obtained CEF levels. The anisotropic molecular fields corresponding to the antiferromagnetic exchange interaction may be expected to affect the large anisotropy of $\chi(T)$. To confirm this assumption, the anisotropy of $\chi(T)$ is necessary to be reproduced by using all CEF terms based on the CEF levels which is determined by the inelastic neutron scattering measurement.

Next, We discuss the low temperature properties. The antiferromagnetic transition in YbCuGe is evidenced by the sharp peak of $C(T)$, the shoulder of χ_a, and the hump of χ_c at 4.2 K, in contrast to the predicted ferromagnetic ordering below 8 K. In the previous report, a few amount of several unknown phases was identified from the X-ray diffraction patterns of the polycrystalline YbCuGe [3]. $Lu_3Cu_4Ge_4$ phase easily precipitates in the LuCuGe sample synthesized in this time. Therefore, we suppose that the previous YbCuGe sample was contaminated with $Yb_3Cu_4Ge_4$ phase, and the sudden rise of $\chi(T)$ below 8 K was ascribed to the ferromagnetic ordering of $Yb_3Cu_4Ge_4$ with $T_C = 7.5$ K [15]. Furthermore, we suppose that the ordered magnetic moments of YbCuGe point the opposite way along the *c*-axis. However, χ_c is gradually decreasing below T_N as compared with the representative antiferromagnet MnF_2 with magnetic structure of single-***k*** [16]. Probably, anisotropic exchange interaction which acts on single ion anisotropy extracted from the CEF effect at Yb site plays important role. The investigation of the magnetic structure will be desired by the elastic neutron diffraction measurements.

In addition to the previous discussion, we consider the expanded tail of $C(T)$ above T_N which recovers the entropy of *R*ln2 in YbCuGe. Because of the small γ value, the suppression of entropy gain can not be explained by the Kondo effect [1]. Then, we propose that the large tail of $C(T)$ above T_N results from geometrical magnetic frustration due to the competition of exchange interaction within the quasi-two dimensional Yb plane, which forms the triangle arrangement of Yb ions in the Yb sublattice sandwiched between the honeycomb Cu–Ge planes. Recently, it is evidenced that frustration arising from the triangular geometry of the magnetic sublattice, impedes long range ordering in antiferromagnetic heavy-fermions such as CePdAl and YbAgGe [17–19]. Both compounds crystallize in the ZrNiAl-type hexagonal structure where rare-earth ions in the *c*-plane form a Kagomé lattice. The frustrated antiferromagnetic interaction is originated from a hexagonal coordination of Kagomé symmetry. However, the ground state of YbCuGe is not heavy. The Yb ions occupy a simple triangle array. Therefore, we suggest that YbCuGe is a candidate to study a standard geometrical frustration effect in magnetic metal. Physical property measurements under high pressure may confirm our assumption.

5. Conclusions

The magnetic and transport properties of single-crystal of YbCuGe are presented. The magnetic susceptibility which shows uniaxial anisotropic behavior along the *c*-axis in all temperature range has a kink at around 4.2 K. The specific heat also shows a λ-type peak at 4.2 K, which decays toward low temperature side by an application of the magnetic field up to 90 kOe. The linear specific heat coefficient is estimated to be 5.2 mJ/mol K^2 from the zero field data. The electrical resistivity for the current along the principal axes shows a metallic behavior with a broad maximum at around 200 K. The Hall coefficient drastically changes from the negative minimum at 70 K to the positive constant value below 10 K. The carrier concentration is estimated to be 0.1/f.u. from the Hall coefficient at 2 K. These results indicate that YbCuGe is a metallic antiferromagnet with $T_N = 4.2$ K.

References

[1] N. Grewe, F. Steglich, in: K.A. Gschneidner Jr., L. Eyring (Eds.), Handbook on the Physics and Chemistry of Rare Earths, vol. 14, North-Holland, Amsterdam, 1991, pp. 343–474.
[2] R. Pöttgen, D. Johrendt, D. Kußmann, in: K.A. Gschneidner Jr., L. Eyring (Eds.), Handbook on the Physics and Chemistry of Rare Earths, vol. 32, North-Holland, Amsterdam, 2001, pp. 453–513.
[3] K. Katoh, Y. Mano, K. Nakano, G. Terui, Y. Niide, A. Ochiai, J. Magn. Magn. Mater. 268 (2004) 212.
[4] K. Katoh, T. Tsutsumi, K. Yamada, G. Terui, Y. Niide, A. Ochiai, Physica B 369 (2005) 81.
[5] K. Katoh, S. Nakagawa, G. Terui, A. Ochiai, J. Phys. Soc. Jpn. 78 (2009) 104721.
[6] K. Katoh, T. Koga, G. Terui, A. Ochiai, J. Phys. Soc. Jpn. 79 (2010) 084709.
[7] M. Kasaya, T. Tani, K. Kawate, T. Mizushima, Y. Ishikawa, K. Sato, J. Phys. Soc. Jpn. 60 (1991) 3145.
[8] P. Bonville, P. Bellot, J.A. Hodges, P. Imbert, G. Jéhanno, G.L. Bras, J. Hammann, L. Leylekian, G. Chevrier, P. Thuéry, L. D'Onofrio, A. Hamzic, A. Barthélémy, Physica B 182 (1992) 105.

[9] B. Heying, U.C. Rodewald, R. Pöttgen, K. Katoh, Y. Niide, A. Ochiai, Monatshe. Chem. 136 (2005) 655.
[10] K. Katoh, T. Takabatake, I. Oguro, A. Ochiai, A. Uesawa, T. Suzuki, J. Phys. Soc. Jpn. 68 (1999) 613.
[11] A.J. Arko, G. Crabtree, D. Karim, F.M. Muellr, L.R. Windmiller, J.B. Ketterson, Z. Fisk, Phys. Rev. B 13 (1976) 5240.
[12] C.M. Hurd, The Hall Effect in Metals and Alloys, Plenum Press, New York, 1972, p. 101.
[13] R. Kubo, Phys. Rev. 87 (1952) 568.
[14] U. Walter, J. Phys. Chem. Solids 45 (1984) 401.
[15] S.K. Dhar, S. Singh, P. Bonville, C. Mazumdar, P. Manfrinetti, A. Palenzona, Physica B 312–313 (2002) 846.
[16] F. Keffer, Phys. Rev. 87 (1952) 608.
[17] A. Dönii, G. Ehlers, H. Maletta, P. Fischer, H. Kitazawa, M. Zolliker, J. Phys.: Condens. Matter 8 (1996) 11213.
[18] P. Bonville, M. Rams, K. Królas, J.-P. Sanchez, P.C. Canfield, O. Trovarelli, C. Geibel, Eur. Phys. J. B 55 (2007) 77.
[19] K. Sengupta, M.K. Forthaus, H. Kubo, K. Katoh, K. Umeo, T. Takabatake, M.M. Abd-Elmeguid, Phys. Rev. B 81 (2010) 125129.